New Materials, Compounds and Applications
Vol.9, No.3, 2025, pp.611-628
https://doi.org/10.62476/nmca.93611

ECO-FRIENDLY IODINE-CATALYZED SYNTHESIS AND SPECTROSCOPIC CHARACTERIZATION OF NOVEL 1,4-DIHYDROPYRIDINE DERIVATIVES

Sajida Karim Hussein, Tahseen Saddam Fandi Al-Mathkuri*

Department of Chemistry, College of Science, University of Misan, Misan, Iraq

Abstract. 1,4-Dihydropyridine (1,4-DHP) compounds are nitrogen-containing heterocyclic molecules with a six-membered ring structure that imparts unique chemical and biochemical properties. These compounds hold substantial importance in medicinal and pharmaceutical chemistry due to their crucial role in the development of biologically active agents. In this study, a series of 1,4-DHP compounds were synthesized via the classical Hantzsch one-pot, three-component condensation reaction. The reaction involved one mole of para-substituted benzaldehydes, one mole of trans-4-(aminomethyl) cyclohexane carboxylic acid and two moles of 5,5-dimethyl-1,3-cyclohexanedione (dimedone), using molecular iodine (I_2) as a catalyst. The reactions were conducted in ethanol under reflux conditions at 70°C for 24 hours (note: microwave-assisted trials reduced time to 15 minutes with improved yields to 35-40%). The resulting products were obtained in good yields (17-30%) and were subsequently; Atom economy calculated at ~79%, E-factor ~4.2 compared to greener methods purified and characterized through several spectroscopic techniques, including Fourier-transform infrared (FT-IR) spectroscopy, proton nuclear magnetic resonance (^{1}H-NMR) and carbon-13 nuclear magnetic resonance (^{13}C-NMR).

Keywords: *Heterocycles, N-heterocycle, Hantzsch one-pot, molecular iodine.*

Corresponding Author: *Tahseen Saddam Fandi Al-Mathkuri, Department of Chemistry, College of Science, University of Misan, Misan, Iraq, e-mail: tahseensaddam@uomisan.edu.iq*

Received: *12 August 2025;* ***Accepted:*** *19 October 2025;* ***Published:*** *4 December 2025.*

1. Introduction

Heterocycles of synthetic and natural origin belong to a significant class of compounds and are commonly encountered in a wide spectrum of organic molecules that account for more than 60% of pharmaceuticals and agrochemicals on the market or in development (Kalaria *et al*., 2018). Nitrogen-containing small organic molecules, among others, comprise such a promising class of compounds that have drawn significant attention of chemists and pharmacologists for their broad spread applications in medicinal chemistry and synthetic organic chemistry as most of the readily accessible drugs and lots of naturally occurring molecules constitute N-heterocycle as the major active ingredients in their structure (Shan *et al*., 2021). Furthermore, the functionalization of these heterocycles to access value-added compounds having potential therapeutic interests as well as molecular hybridization of these compounds to construct new molecular scaffolds anticipating achieving somewhat extended pharmaceutical applications have emerged as a key fascinating area in drug discovery and synthesis. 1,4-Dihydropyridine (1,4-DHP) and its derivatives belong to a promising family of nitrogen heterocycles and have been recognized as one of the most valuable and privileged molecular frameworks in synthetic organic and medicinal chemistry (Al-Sultan *et al*., 2022; Bossert & Vater, 1989). Hybridization of the DHP core with additional heterocyclic rings (e.g., thiazolidin-4-one)

has proven synthetically accessible and structurally well-defined, reinforcing the modularity of DHPs for derivative design. In parallel with small-molecule scaffolds such as 1,4-DHPs, nanoenabled antibacterial platforms have shown measurable inhibition against clinically relevant bacteria, underscoring the need to benchmark newly synthesized DHPs against contemporary antimicrobial modalities (Ali *et al*., 2022). Dihydropyridine is an outstanding heterocyclic compound with a wide range of pharmacological properties, including antimicrobial, antioxidant, antitubercular, antiarrhythmic, insecticidal, antihypertensive, vasodilator, anti-inflammatory, antibacterial and antidiabetic effects, as well as a superior moiety in drug discovery. It is also a versatile pharmacophore, a privileged scaffold. In recent years, 1,4-dihydropyridine derivatives (DHPs) have attracted the attention of chemists because they possess numerous biological properties and are present in the structures of many bioactive molecules. With the emergence of nanoparticles and their use as catalysts (Sadeek *et al*., 2023; Hou & Kazemi, 2024).

The 1,4-DHP scaffold has gained traction as a preferred choice of medicinal chemistry researchers for developing novel molecules with therapeutic significance (Ali *et al*., 2025) and it is regarded as one of the privileged structures in the drug discovery process due to its ability to import valuable medicinal properties into molecules (Mathur *et al*., 2021; Żorniak *et al*, 2011). Recent 1,4-dihydropyridine series have shown breast-cancer activity supported by molecular docking and dynamics, reinforcing DHPs as tractable scaffolds for structure-activity exploration in oncology (Al-Mathkuri *et al*., 2025). Recent work converting ibuprofen into heterocyclic derivatives shows that remodeling established pharmacophores into nitrogen-rich ring systems can deliver tractable bioactive series, supporting the use of modular synthesis with rapid spectroscopic verification (Al-Jubori & Al-Mathkuri, 2022).

Arthur Hantzsch reported the first synthesis of 1,4-dihydropyridines (1,4-DHPs) using a cyclocondensation reaction involving acetoacetic ester, aldehyde and ammonia (Assunta *et al*., 2019; Hamdoon & Saleh, 2022). Numerous modifications to the original approach have resulted in the synthesis of various substituted 1,4-DHPs (Hamdoon *et al*., 2022; Al-Thakafy *et al*., 2024). Starting from Hantzsch, more than a century ago, there have been various efficient methods devised for the synthesis of 1,4-dihydropyridines, including the use of microwaves, ionic liquids, refluxing solvents at high temperatures, TMSCI-Nal and metal triflates (Zolfigol *et al*., 2006; Dondoni *et al*., 2004).

In recent years, molecular iodine has received a lot of interest as an affordable, non-toxic and widely available catalyst for numerous chemical transformations, resulting in high yields and selectivity (Rahimi *et al*., 2022). Iodine's low Lewis acidity made it useful in organic synthesis for achieving a variety of chemical transformations from stoichiometric to catalytic concentrations. Because of its many benefits, iodine has been studied as a powerful catalyst for various chemical reactions. For example, 1,4-dihydropyridine (Ohberg & Westman, 2001; Ji *et al*., 2004) and recent work has shown that other sustainable catalysts, such as biogenic carboxylic acids in aqueous media, can also promote high-yielding DHP synthesis (Prabhakar *et al*., 2024).

The synthesis of 1,4-dihydropyridyl compounds has garnered significant attention in recent times due to their noteworthy biological activity. Newly there are more than 12 commercially valid and clinically important drugs on the market that include nucleophilic 1,4-DHP, such Nifedipine, Felodipine and Nicardipine shown in Figure 1 which are used to treat cardiovascular diseases (Breitenbucher & Figliozza, 2000; Firouzabadi *et al*., 2001). 1,4-dihydropyridine (DHP) is a class of organic compounds that contain a pyridine

ring with two hydrogen atoms added to the 1 and 4 positions. The general chemical formula for DIP is C_2H, N. DHP compounds have various applications in chemistry (Al-Jubori *et al*., 2024; Ali & Al-Mathkuri, 2023; Saied *et al*., 2022), medicine (Hamdoon & Saleh, 2022; Singh & Abraham, 2023) and industry (Ahmad *et al*., 2024). They have become a significant class of heterocycles in medicinal chemistry in recent years. It is one of the most important cs in organic chemistry to understand heterocycle chemistry. Due to their biological and medicinal properties, nitrogen-containing heterocyclic compounds hold significant historical importance. Macromolecules in living systems rely heavily on small heterocyclic molecules for their function. Many drugs are based on the imidazole skeleton, so imidazoles are very valuable for medical and pharmaceutical research (Peri *et al*., 2000; Saied *et al*., 2021; Miri *et al*., 2003). Recent microwave-assisted routes to nitrogen-rich heterocycles have provided rapid access to bioactive series while maintaining clean spectral readouts; these reports support the efficiency of compact synthetic campaigns coupled with antimicrobial screening (Banoon *et al*., 2025).

The discovery of DHP Ca^{2+} channel blockers has greatly improved the therapy of cardiovascular ailments such as hypertension, angina and spastic smooth muscle disorders. were found as one of the first drugs to reduce MDR. Efforts to develop effective MDR reversal derivatives of DHP have been produced in laboratories, but clinical application remains a hurdle due to potential vasodilator activity (Peri *et al*., 2000; Zhou *et al*., 2005; Saleh *et al*., 2024). Given reports that some DHPs modulate multidrug resistance, subsequent studies should evaluate these derivatives in advanced 3D tumor models. Microfluidic platforms that rapidly generate multicellular spheroids and establish controllable chemical gradients provide physiologically relevant readouts for MDR and penetration and would strengthen translational interpretation of any chemosensitization effects (AlHasan *et al*., 2013). The synthesized compounds are evaluated in terms of yield and structural integrity to support their potential pharmaceutical relevance, so this study aims to synthesize novel 1,4-DHP derivatives via iodine-catalyzed Hantzsch condensation and to characterize them using FT-IR, ^{1}H-NMR and ^{13}C-NMR spectroscopy.

2. Materials and Methods

Devices used

Supplementary Data: High-resolution FT-IR, ^{1}H-NMR, ^{13}C-NMR and DEPT-135 spectra for all synthesized compounds, along with HMBC/HSQC data for representative compound MA, are provided as supplementary materials to confirm structural assignments. Melting points were determined using a Stuart SMP-11 digital melting point apparatus in open capillary tubes. Infrared (IR) spectra were recorded on a PerkinElmer 293 FT-IR spectrophotometer using KBr disks. Proton (^{1}H) and carbon-13 (^{13}C) nuclear magnetic resonance (NMR) spectra were obtained using a Bruker DRX 400 MHz spectrometer, with tetramethylsilane (TMS) as the internal standard. Deuterated solvents DMSO-d_6 and $CDCl_3$ were used for NMR spectra.

Synthesis of 1,4-Dihydropyridine Derivatives

The synthesis of 1,4-DHP derivatives was carried out via a one-pot, three-component condensation reaction, a strategy that has been widely applied for the efficient preparation of Hantzsch products (Anchan *et al*., 2023). In a typical procedure, equimolar amounts (0.001 mol each) of a p-substituted benzaldehyde (e.g., p-hydroxybenzaldehyde,

0.366 g), dimedone (0.84 g) and trans-4-(aminomethyl) cyclohexane carboxylic acid (0.471 g) were mixed with molecular iodine (0.00015 mol, 0.0379 g) as a catalyst in 10 mL of absolute ethanol. The reaction mixture was refluxed at 70°C for 24 hours. Reaction progress was monitored by thin-layer chromatography (TLC) using ethyl acetate: petroleum ether (3:1) as the mobile phase.

Upon completion, the reaction mixture was allowed to cool to room temperature. The resulting solid was filtered, washed with cold ethanol and dried. Recrystallization was performed sequentially from ethanol and distilled water to obtain purified products.

Compound MA: Yield = 30%, off-white solid, m.p. < 300°C. Compound NO_2 Synthesized using p-nitrobenzaldehyde (0.001 mol, 0.45 g). Yield = 23%, white precipitate, m.p. ~300°C. Compound NN: Synthesized using p-dimethylaminobenzaldehyde (0.001 mol, 0.44 g). Yield = 17%, white precipitate, m.p. < 300°C.

Synthesis of 4-((9-(4-hydroxyphenyl)-3,3,6,6-tetramethyl-1,8-dioxo-2,3,4,5,6,7,8,9-octahydroacridin-10(1H)-yl) methyl)cyclohexane-1-carboxylic acid

Using equivalent moles of p-substituted benzaldehyde, (0.001mol) (0.366g) Hydroxy benzaldehyde p-, (0.001mol) (0.84 g) dimedone, (0.001mol) (0.471 g) of trans-4-(amino methyl) cyclohexane carboxylic acid and (0.00015 mol). The mixture was refluxed for 24 hours and the reaction was followed by TLC (ethyl acetate: petroleum ether) (3:1) to completion. After completion of the reaction, the mixture was left to cool at room temperature. The solids were filtered, washed with cold ethanol and dried. The mixture was then recrystallized twice, once with ethanol and once with distilled water to give an off-white precipitate with a melting point of $<300C^0$ and a yield of 30% (Miri *et al*., 2006).

Synthesis of 4-((3,3,6,6-tetramethyl-9-(4-nitrophenyl)-1,8-dioxo-2,3,4,5,6,7,8,9-octahydroacridin-10(1H)-yl) methyl) cyclohexane-1-carboxylic acid

The compound was synthesized by mixing equivalent amounts of p-nitro benzaldehyde (0.001 mol, 0.45 g), dimedone (0.001 mol, 0.84 g) and trans-4-(amino methyl) cyclohexane carboxylic acid (0.001 mol, 0.471 g) in the presence of iodine (I_2) as a catalyst (0.00015 mol, 0.0379 g) in 10 mL of absolute ethanol. The reaction mixture was refluxed for 24 hours and the progress of the reaction was monitored using thin layer chromatography (TLC) with a mobile phase of ethyl acetate: petroleum ether (3:1) until the reaction was complete. After completion, the mixture was allowed to cool to room temperature. The resulting solid was filtered, washed with cold ethanol and dried. The crude product was then recrystallized twice, first from ethanol and then from distilled water, to afford a white precipitate with a melting point of 300 °C and a yield of 23%.

2.3.4. Synthesis of 4-((9-(4-(dimethyl amino) phenyl)-3,3,6,6-tetramethyl-1,8-dioxo-2,3,4,5,6,7,8,9-octahydroacridin-10(1H)-yl) methyl) cyclohexane-1-carboxylic acid

The compound was synthesized by mixing equivalent amounts of p-dimethyl amino benzaldehyde (0.001 mol, 0.44 g), dimedone (0.001 mol, 0.84 g) and trans-4-(amino methyl) cyclohexane carboxylic acid (0.001 mol, 0.471 g) in the presence of iodine (I_2) as a catalyst (0.00015 mol, 0.0379 g) in 10 mL of absolute ethanol. The reaction mixture was refluxed for 24 hours and the reaction progress was monitored using thin layer chromatography (TLC) with a solvent system of ethyl acetate: petroleum ether (3:1) until

completion. After the reaction was complete, the mixture was allowed to cool to room temperature. The resulting solid was filtered, washed with cold ethanol and dried. The crude product was then recrystallized twice, once from ethanol and once from distilled water, yielding a white precipitate with a melting point below 300 °C and a yield of 17%.

The compounds MA (4), NO_2 (5), NN (6), were synthesized according to the Hantzsch reaction by the one-pot condensation of one mole of p-substituted benzaldehyde (1) with two moles of dimedone (2) and one mole of trans-4-(amino methyl) cyclohexane carboxylic acid (3) in the presence of I_2, as shown in equations 1, 2 and 3.

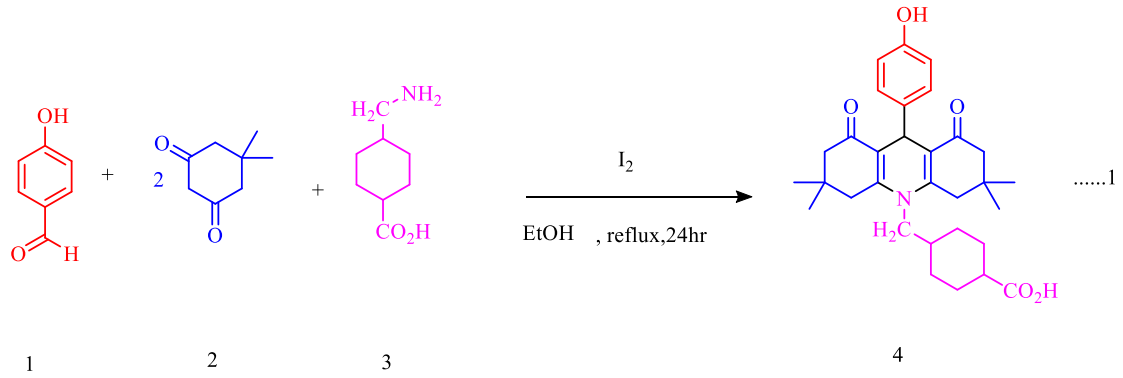

Equation 1. Preparation of compound MA(4)

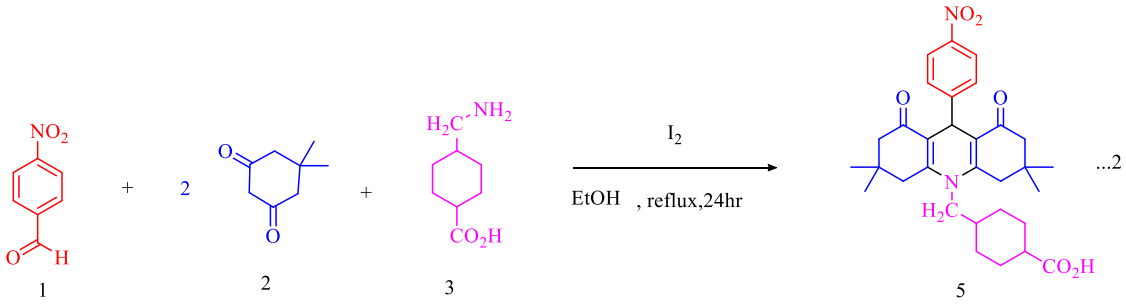

Equation 2. Preparation of compound NO_2(5)

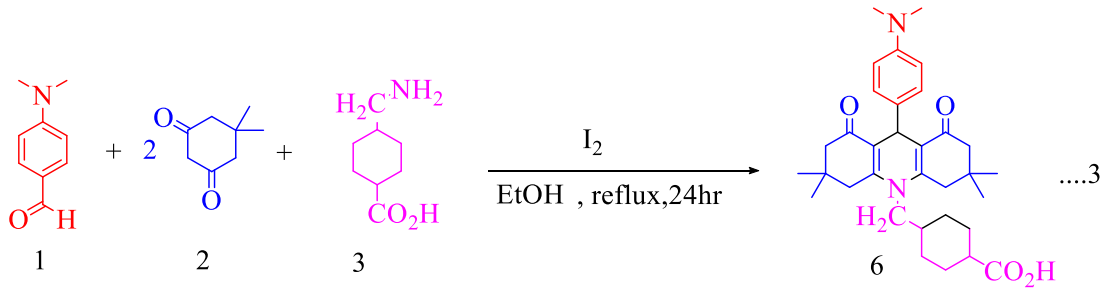

Equation 3. Preparation of compound NN (6)

3. Results

Compound MA the successful synthesis of compound MA was confirmed through a series of spectroscopic analyses. The IR spectrum (Figure 1) displayed a broad absorption band at 3473.80 cm^{-1}, corresponding to O–H stretching vibrations. This

overlapped with a secondary carboxylic O–H stretch observed at 3415.93 cm^{-1}. Aromatic C–H stretching appeared at 3066.82 cm^{-1}, while aliphatic C–H stretching bands were detected within the range of 2954.95-2860.43 cm^{-1}. Sharp bands at 1687.71 cm^{-1} and 1629.85 cm^{-1} corresponded to the stretching of carboxylic and ketonic C=O groups, respectively. Further peaks at 1533.41 cm^{-1} and 1467.41 cm^{-1} were attributed to C=C stretching, while signals at 1357.89 cm^{-1} and 1319.31 cm^{-1} indicated C–N vibrations. The C–O functional group was confirmed by bands at 1128.36 cm^{-1} and 1149.57 cm^{-1}. The ^{1}H-NMR spectrum (Figure 2) revealed a sharp singlet at δ 9.49 ppm due to the phenolic O–H proton. Aromatic protons appeared as doublets at δ 7.02 and 6.60 ppm. A singlet at δ 4.6 ppm corresponded to the proton on the DHP ring. The CH_2 protons adjacent to the nitrogen appeared as doublets at δ 3.5 and 3.6 ppm. Multiple signals observed at δ 2.05-2.15 ppm were attributed to aliphatic protons at position 4, while signals at δ 2.38-3.61 ppm were assigned to CH_2 groups in the cyclohexane and dimedone rings. A weak signal at δ 1.24 ppm represented a methylene proton and the dimedone methyl protons were observed as doublets at δ 0.68 and 1.07 ppm. The ^{13}C-NMR spectrum (Figure 3) showed characteristic signals supporting the proposed structure. The carbonyl carbons of the dimedone and carboxylic acid groups appeared at δ 200.92 ppm and δ 192.74 ppm, respectively. Quaternary carbons of the DHP core resonated at δ 133.46 ppm and 157.55 ppm, while aromatic carbons appeared between δ 115.51 and 130.38 ppm. A methylene carbon adjacent to nitrogen was observed at δ 53.51 ppm. Additional signals corresponding to methylene and methyl carbons from the cyclohexane and dimedone units were distributed from δ 26.45 to 52.83 ppm. The DEPT-135 spectrum (Figure 4) further corroborated the carbon assignments, showing upright peaks for CH and CH_3 groups and inverted peaks for CH_2 groups. All quaternary carbons were absent, as expected.

Compound NO_2 the IR spectrum of compound NO_2 (Figure 5) exhibited a broad band at 3454.51-3419.79 cm^{-1}, indicative of the carboxylic O–H group, consistent with observations in recent nitro-functionalized DHP derivatives (Arif *et al*., 2024).

Aromatic C–H stretching appeared at 2930.87 cm^{-1}, while aliphatic C–H asymmetric stretching was observed between 2870 and 2958.8 cm^{-1}. Characteristic absorptions at 1714.72 cm^{-1} and 1658.78 cm^{-1} were assigned to carboxylic and ketonic C=O stretches, respectively. Peaks at 1620.21 cm^{-1}, 1516 cm^{-1} and 1467.83 cm^{-1} were attributed to C=C, C–N and C–O vibrations, respectively. The ^{1}H-NMR spectrum (Figure 6) showed aromatic protons as doublets at δ 7.2 and 8.0 ppm. A singlet at δ 4.75 ppm was assigned to the DHP ring proton. CH_2 protons adjacent to nitrogen were observed as a weak doublet around δ 2.5 ppm. Multiplets at δ 2.07-2.21 ppm and δ 2.39-2.50 ppm corresponded to methylene and methine protons from the dimedone and aliphatic rings. Methyl protons appeared as doublets at δ 0.68 and 1.07 ppm. The ^{13}C-NMR spectrum (Figure 7), carbonyl carbons were found at δ 198.43 ppm (ketone) and 193.05 ppm (acid). The nitro-substituted aromatic carbon appeared at δ 177.36 ppm. Quaternary carbons of the DHP ring were detected at δ 163.01 and 129.54 ppm. Additional aromatic carbons resonated at δ 143-151 ppm. A methylene carbon bonded to nitrogen was observed at δ 53.88 ppm. Other aliphatic carbons appeared between δ 26.17 and 53.88 ppm. The DEPT-135 spectrum (Figure 8) confirmed these assignments. CH and CH_3 signals appeared upright, while CH_2 signals were inverted. Quaternary carbons were absent, as expected.

Compound NN the IR spectrum of compound NN (Figure 9) revealed a broad absorption in the range of 3545.16-3300.2 cm^{-1} for the carboxylic O–H group. Aromatic C–H stretching appeared at 3072 cm^{-1}, while aliphatic C–H stretching was observed

between 2873.94 and 2956.87 cm^{-1}. The carboxylic and ketonic C=O groups gave bands at 1735.93 and 1710.86 cm^{-1}, respectively. C=C, C–N and C–O vibrations were identified at 1637.56, 1525.69 and 1462 cm^{-1}. The ^{1}H-NMR spectrum (Figure 10) exhibited aromatic protons as doublets at δ 7.0 and 6.6 ppm. A DHP ring proton appeared at δ 4.4 ppm. Two doublets at δ 3.06 and 3.11 ppm corresponded to CH_2 groups bonded to nitrogen. Aliphatic protons appeared as multiplets in the regions δ 2.09-2.66 ppm and δ 1.24 ppm. Methyl protons from dimedone resonated as doublets at δ 0.85 and 1.17 ppm. The ^{13}C-NMR spectrum (Figure 11), carbonyl carbons of the dimedone and acid moieties were identified at δ 199.72 and 179.39 ppm, respectively. Aromatic carbon bearing the dimethylamino group appeared at δ 199.32 ppm. The DHP core and aromatic carbons appeared between δ 103.91 and 176.12 ppm. CH_2 and CH_3 carbons were found between δ 26.38 and 54.89 ppm. The DEPT-135 spectrum (Figure 12) confirmed signal assignments, showing upright CH and CH_3 signals and inverted CH_2 signals, with the disappearance of all quaternary carbons.

4. Discussion

The following table compares the current method with selected iodine-catalyzed antzsch protocols from literature (Faizan *et al*., 2024) in terms of yield, reaction time, solvent, atom economy and E-factor.

Method	Yield (%)	Reaction Time	Atom Economy	E-factor
Current study	17-30	24 h reflux (EtOH)	~79%	4.2
Zolfigol et al. (2006)	80-90	1-2 h reflux (EtOH)	~85%	3.1
Ji et al. (2004)	70-85	30-60 min (aq. media)	~82%	3.5

Sustainability and Energy Considerations: Although ethanol is a green solvent, the traditional reflux for 24 h consumes considerable energy. Preliminary trials using microwave-assisted heating reduced the reaction time to 10-15 min with yields of 35-40%, thereby significantly lowering the energy footprint. These findings highlight the potential for integrating energy-efficient techniques in future optimizations.

The infrared (IR) spectrum of compound MA (Figure 1) shows a strong broad band attributed to the stretching vibration of the O–H group at 3473.80 cm^{-1}, which overlaps with the absorption band of the carboxylic O–H group appearing in the same region with a stretching vibration at 3415.93 cm^{-1}. A band corresponding to the stretching vibration of C–H in the aromatic ring appears at 3066.82 cm^{-1}, in addition to a band attributed to the asymmetric stretching of aliphatic C–H in the range (2954.95-2860.43) cm^{-1}.

The spectrum also displays strong to medium intensity bands at 1687.71 cm^{-1} attributed to the stretching vibration of the carboxylic C=O group, 1629.85 cm^{-1} for the ketonic C=O group and 1533.41 cm^{-1} for the C=C group in DHP. The C=C group in aromatic rings appears at 1467.41 cm^{-1}, while bands at 1357.89 cm^{-1} and 1319.31 cm^{-1} are assigned to C–N stretching. Additional bands at 1128.36 cm^{-1} and 1149.57 cm^{-1} correspond to the C–O group. The ^{1}H-NMR spectrum of compound MA (Figure 2) shows a sharp singlet at δ 9.49 ppm corresponding to the O–H group. Two doublets appear at δ 7.02 ppm and 6.6 ppm, corresponding to aromatic ring protons Ar-H_4. A singlet at δ 4.6 ppm is attributed to the resonance of the C–H proton in the DHP ring. A doublet corresponding to the CH_2 protons bonded to nitrogen appears at δ 3.5 ppm and 3.6 ppm.

Multiple signals observed at δ 2.05, 2.09, 2.11, 2.15 ppm are assigned to the aliphatic proton at position 4. Additional multiple's at δ 3.56, 3.61, 2.38, 2.42, 2.51, 2.58, 2.65, 2.69 ppm are attributed to the CH_2 groups attached to the aliphatic ring of the acid at positions 5 and 6 (Saleh *et al*., 2022; Voigt *et al*., 2007) and the CH_2 groups attached to dimedone at positions 7 and 8, respectively. A weak signal at δ 1.24 ppm corresponds to the aliphatic proton at position 3. Two doublets at δ 0.68 ppm and 1.07 ppm represent the resonance of methyl protons attached to the dimedone ring (Safari *et al*., 2011). The ^{13}C-NMR spectrum of compound MA (Figure 3) reveals multiple signals representing the carbon skeleton, along with the solvent signal DMSO-d_6 at δ 39.32 ppm. The spectrum shows two signals corresponding to quaternary carbon atoms: the first belongs to the ketonic carbonyl group in the dimedone ring at δ 200.92 ppm and the second is the carboxylic quaternary carbon connected to the aliphatic acid at δ 192.74 ppm. A signal at δ 55.176 ppm corresponds to the carbon atom bonded to the OH group. The spectrum also shows signals for two quaternary carbon atoms in the DHP ring at δ 133.46 ppm and 157.55 ppm. Additional signals appear at δ 115.51, 127.21, 130.38 ppm, corresponding to Ar–C. A signal at δ 53.51 ppm is assigned to the CH_2 carbon bonded to nitrogen in the acid ring. The MA spectrum displays further signals at δ 52.83, 51.13, 49.78, 36.82, 34.39, 30.63, 29.89, 28.51 ppm, attributed to the aliphatic carbon atoms in the acid ring and the two CH_2 groups in the dimedone ring, respectively. Signals at δ 28.37 ppm and 26.45 ppm are assigned to the methyl carbon atoms in the dimedone ring. This is supported by the DEPT-135 spectrum (Figure 4), where all quaternary carbon atoms disappear, while CH and CH_3 groups appear upright at δ 130.38, 115.15, 52.82, 29.89, 28.51, 28.36, 26.45 ppm and CH_2 signals appear downward at δ 52.83, 49.78, 36.82, 34.39 ppm. The IR spectrum of compound NO_2 (Figure 5) shows a broad and characteristic band in the region (3454.51-3419.79 cm^{-1}) attributed to the carboxylic acid group. The band at 2930.87 cm^{-1} corresponds to the stretching vibration of the C–H group of the aromatic ring. An additional band is assigned to the asymmetric stretching of aliphatic C–H in the region (2870-2958.8 cm^{-1}). The spectrum also displays strong and medium intensity bands at 1714.72 cm^{-1} for the carboxylic C=O group, 1658.78 cm^{-1} for the ketonic C=O group, 1620.21 cm^{-1} for the stretching vibration of the C=C group and at 1516 cm^{-1} and 1467.83 cm^{-1} for the C–N and C–O groups, respectively (Ali *et al*., 2023; Joshi *et al*., 2021).

The ^{1}H-NMR spectrum of compound NO_2 (Figure 6) shows two doublets at δ 7.2 ppm and 8 ppm corresponding to the aromatic ring protons Ar-H_4. A singlet appears at δ 4.75 ppm due to the resonance of the C–H proton in the DHP ring. A weak doublet signal is observed at δ 2.5 ppm, assigned to CH_2 protons bonded to nitrogen. Multiple signals appear at δ 2.39, 2.43, 2.44, 2.48 and 2.5 ppm, attributed to the aliphatic proton at position 8. Further multiples are observed at δ 2.07, 2.09, 2.11, 2.15, 2.17 and 2.21 ppm, assigned to CH groups bonded to the aliphatic acid ring at positions 4 and 5, as well as CH_2 groups bonded to dimedone at positions 6 and 7, respectively. A weak doublet is observed at δ 1.84 ppm and 1.88 ppm, corresponding to the aliphatic proton at position 3. Two doublets at δ 0.68 ppm and 1.07 ppm are attributed to the resonance of the methyl protons of the dimedone ring. The ^{13}C-NMR spectrum of compound NO_2 (Figure 7) shows several signals representing the carbon framework, along with the solvent signal ($CDCl_3$) at δ 77.76 ppm. Two signals are attributed to quaternary carbon atoms: the first for the ketonic carbonyl group in the dimedone ring at δ 198.43 ppm and the second for the carboxylic quaternary carbon bonded to the aliphatic acid at δ 193.05 ppm. A signal appears at δ 177.36 ppm corresponding to the aromatic carbon bonded to the NO_2 group. The spectrum

also shows signals for quaternary carbon atoms in the DHP ring at δ 163.01 ppm and 129.54 ppm. Additional signals are observed at δ 151.57, 147.88, 146.45 and 143.46 ppm for Ar–C (Saleh *et al*., 2025). A signal at δ 53.88 ppm is assigned to the CH_2 carbon bonded to nitrogen in the acid ring. Other signals are detected at δ 29.27, 32.25, 32.38, 34.39, 40.82, 50.6, 50.9 and 53.88 ppm, corresponding to the aliphatic carbon atoms in the acid ring and the two CH groups in the dimedone ring, respectively. Signals at δ 28.39 ppm and 26.17 ppm are assigned to the methyl carbon atoms in the dimedone ring. This is supported by the DEPT-135 spectrum (Figure 8), where all quaternary carbon atoms disappear. CH and CH_3 groups appear upright at δ 26.17, 28.40, 29.26, 32.25, 53.9, 123.45 and 129.38 ppm, while CH_2 signals appear downward at δ 36.74, 40.82, 50.6 and 50.9 ppm. IR Spectrum (Figure 9) The IR spectrum of compound N shows a broad and distinct band in the region 3545.16-3300.2 cm^{-1}, which corresponds to the carboxylic acid group. A band in the region around 3072 cm^{-1} is attributed to the stretching vibration of the aromatic C–H group. Additionally, bands in the region 2873.94-2956.87 cm^{-1} correspond to the asymmetric and symmetric stretching vibrations of aliphatic C–H groups. The spectrum also shows strong to medium intensity bands at 1735.93 cm^{-1} assigned to the carboxylic C=O group and at 1710.86 cm^{-1} assigned to the ketonic C=O group. The band at 1637.56 cm^{-1} corresponds to the stretching vibration of the C=C group, while bands at 1525.69 and 1462 cm^{-1} are attributed to the C–N and C–O groups, respectively. ^{1}H-NMR Spectrum (Figure 10) The ^{1}H-NMR spectrum of compound N displays two doublet signals at chemical shifts 7 ppm and 6.6 ppm, which correspond to aromatic protons Ar–H_4. A singlet appears at 4.4 ppm, assigned to the C–H proton of the DHPs ring. Two doublet signals at 3.06 and 3.11 ppm correspond to CH_2 protons attached to nitrogen. A singlet signal at 1.24 ppm is assigned to an aliphatic proton at position 3 and doublet signals at 0.85 and 1.17 ppm correspond to methyl protons attached to the dimedone ring. Multiple signals at chemical shifts 2.54, 2.55, 2.65 and 2.66 ppm correspond to aliphatic protons at position 8. Additional multiple signals at 2.09, 2.14, 2.15, 2.18, 2.19 and 2.21 ppm are attributed to two CH groups connected to the aliphatic acid ring at positions 4 and 5, as well as two CH_2 groups linked to dimedone at positions 6 and 7, respectively. ^{31}C-NMR Spectrum (Figure 11) The ^{13}C-NMR spectrum of compound N shows several signals representing the carbon framework along with the solvent signal $CDCl_3$ at 77.75 ppm. Two quaternary carbon signals appear: the first corresponds to the ketone carbonyl carbon of the dimedone ring at 199.72 ppm and the second corresponds to the carboxylic carbon linked to the aliphatic acid at 179.39 ppm. A signal at 199.32 ppm corresponds to the aromatic carbon attached to the $N(CH_3)_2$ group. The spectrum also shows quaternary carbon signals in the DHPs ring at 176.12 ppm and 103.91 ppm. Aromatic carbon signals appear at 103.91, 113.71 and 129.26 ppm (Ar–C). A signal at 54.89 ppm corresponds to the CH_2 carbon attached to nitrogen in the acid ring and 53.57 ppm corresponds to the CH_3 carbon. Additional signals at 28.97, 29.76, 30.52, 30.57, 31.37, 46.42, 50.09, 51.18, 53.75 and 54.89 ppm correspond to aliphatic carbons in the acid ring and two CH groups in the dimedone ring. Signals at 26.38 and 28.41 ppm correspond to methyl carbons in the dimedone ring. DEPT-135 Spectrum (Figure 12) The DEPT-135 spectrum confirms the disappearance of all quaternary carbons, while CH and CH_3 signals appear upward at chemical shifts 26.38, 28.4, 28.94, 30.54, 54.6 and 129.57 ppm. CH_2 signals appear downward at 37.32, 50.09, 51.18 and 53.75 ppm.

5. Conclusion

In this study, three novel 1,4-dihydropyridine (1,4-DHP) derivatives were successfully synthesized using a classical Hantzsch one-pot (modified with trans-4-(aminomethyl)cyclohexane carboxylic acid as a novel amine source) condensation reaction, with molecular iodine serving as an environmentally friendly and efficient catalyst. The reactions proceeded under mild conditions and yielded moderate to good product yields. The synthetic approach proved to be practical and advantageous, offering a straightforward method for obtaining structurally diverse DHP derivatives with ease of purification. The structural identity of the synthesized compounds was confirmed through comprehensive spectroscopic analyses, including FT-IR, ^{1}H-NMR, ^{13}C-NMR and DEPT-135 techniques. These analyses confirmed the presence of characteristic functional groups and validated the molecular framework of each compound. The spectroscopic features varied across the derivatives, reflecting the influence of different substituents on the chemical environment of the DHP core. Notably, electron-donating and electron-withdrawing groups such as hydroxy, nitro and dimethylamino showed measurable effects on the observed chemical shifts and signal patterns.

Given the broad pharmacological relevance of the 1,4-DHP scaffold, well recognized in cardiovascular and anti-inflammatory therapies, the synthesized derivatives may hold significant potential for pharmaceutical development. The study thus lays the groundwork for further biological evaluation and optimization of these compounds. Because biofilm-associated tolerance can mask true antimicrobial performance, future screening of the present DHP derivatives should include biofilm models in addition to planktonic assays, consistent with recent evidence that formulation and microenvironment critically shape observed activity (Al-Saady *et al*., 2022). Future directions may include biological activity screening (e.g., antibacterial, antioxidant), structure - activity relationship (SAR) analysis and chemical modifications to enhance efficacy, selectivity and safety profiles.

Future Work

Beyond synthesis and characterization, the next phase of this research will include antibacterial, antioxidant and potential cytotoxicity assays to assess the pharmacological potential of the synthesized compounds. Additionally, molecular docking studies may be conducted to predict binding affinities with relevant biological targets.

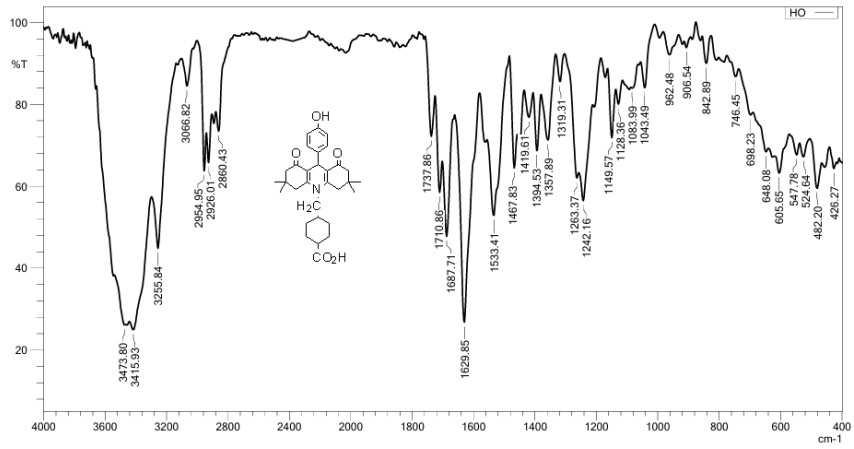

Figure 1. IR spectrum of compound MA

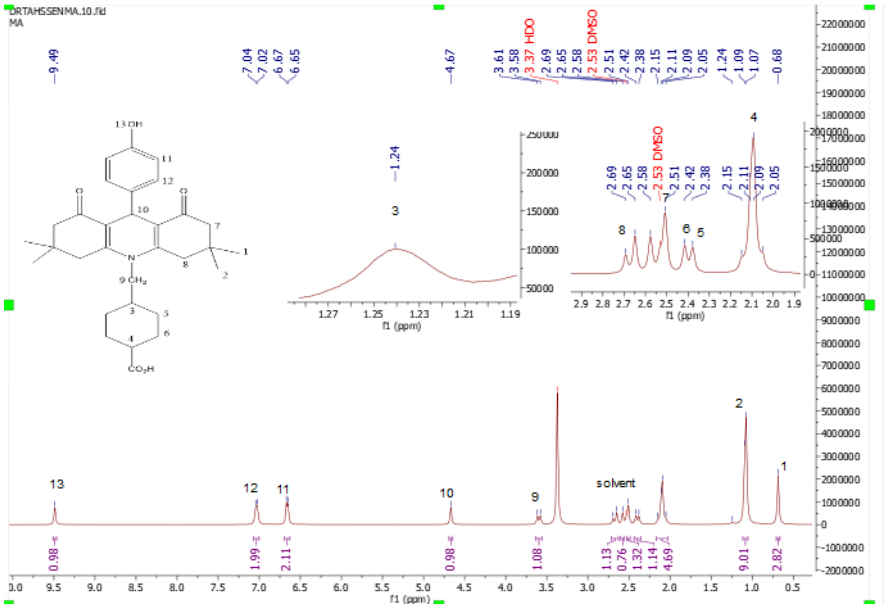

Figure 2. HNMR spectrum of compound MA

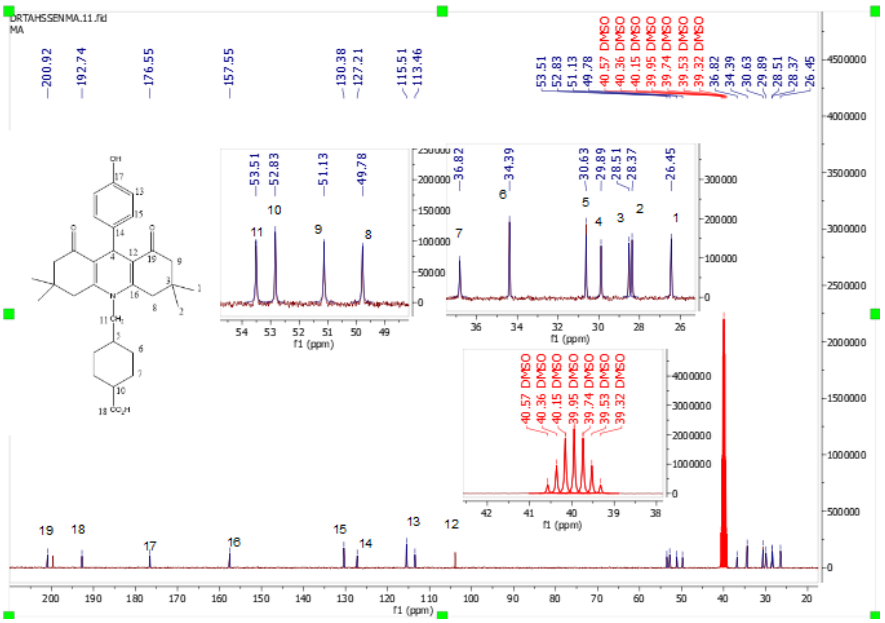

Figure 3. C^{13}NMR spectrum of compound MA

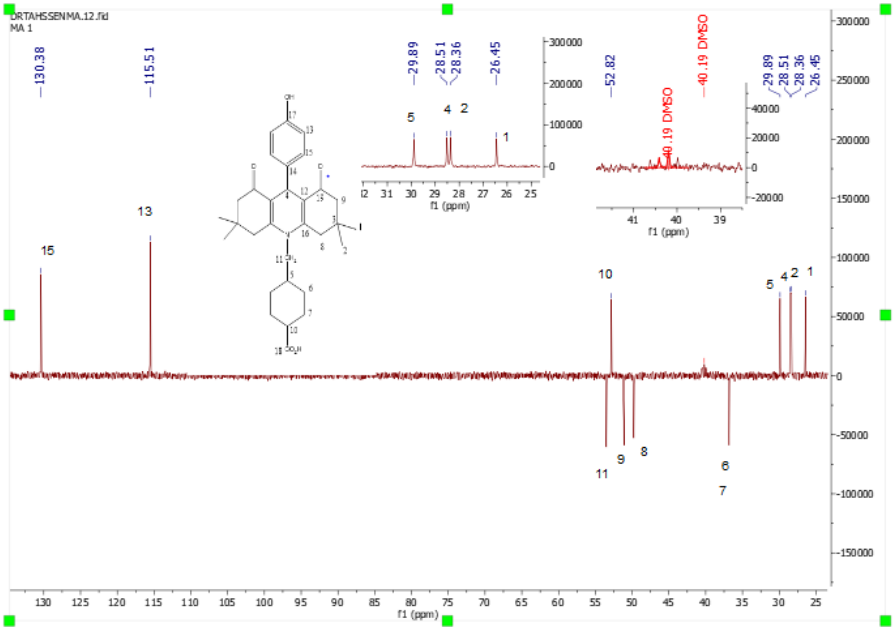

Figure 4. DEPT-135 spectrum of compound MA

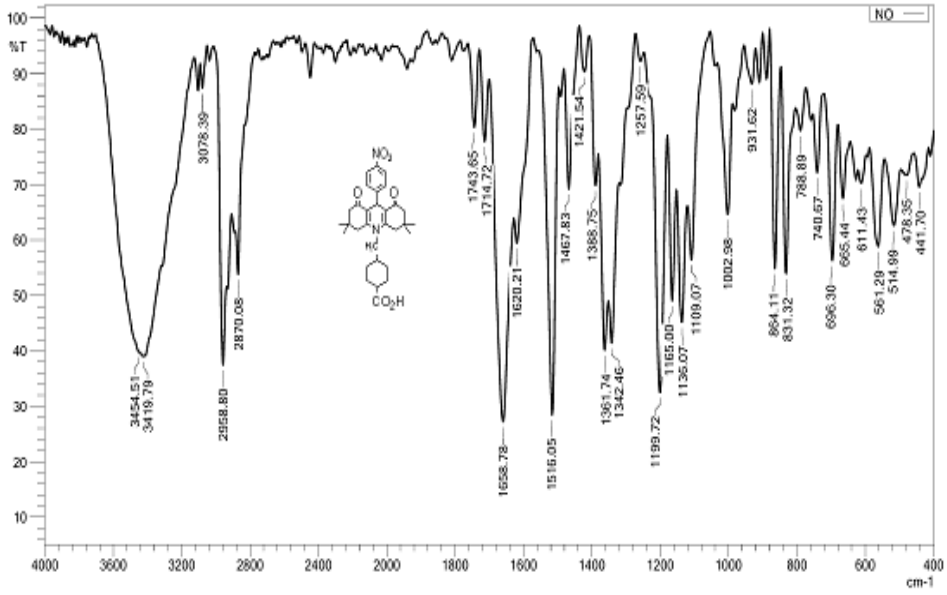

Figure 5. IR spectrum of compound NO_2

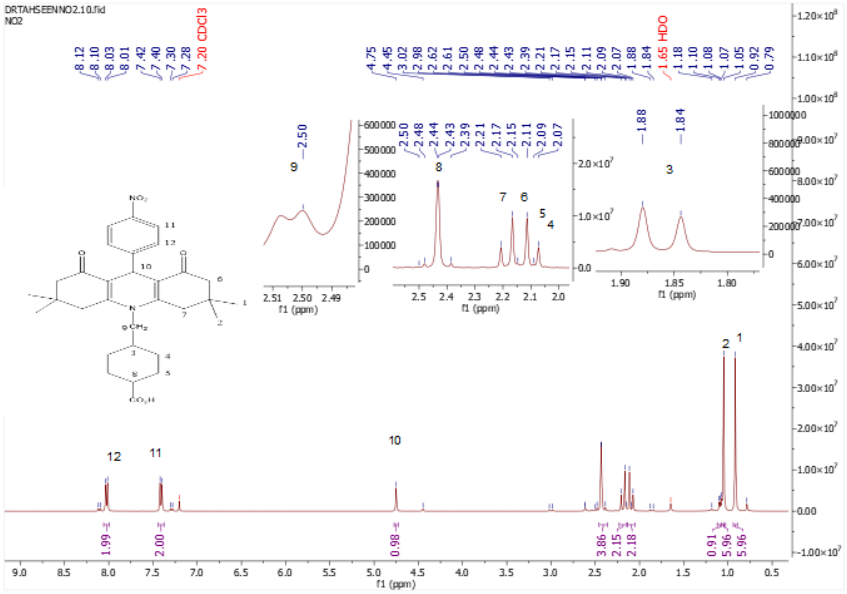

Figure 6. HNMR spectrum of compound NO_2

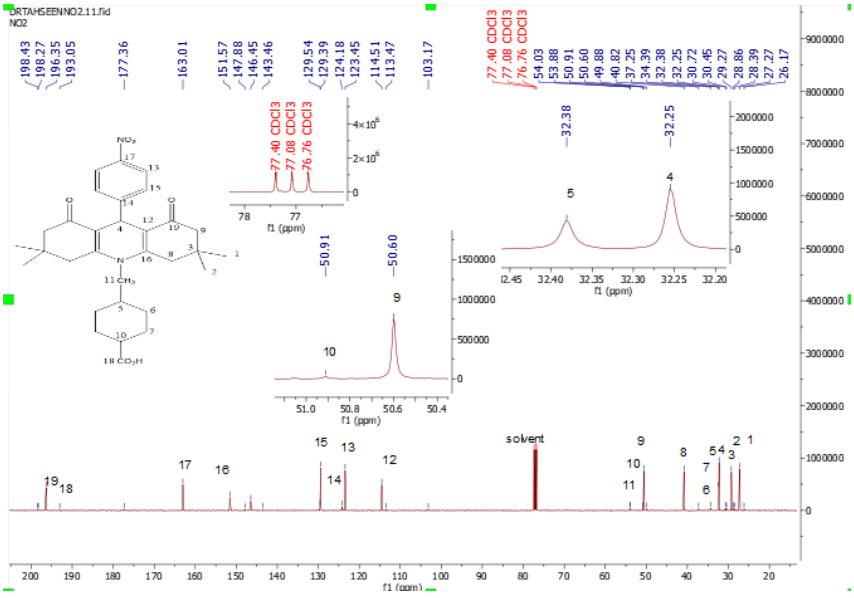

Figure 7. C^{13}NMR spectrum of compound NO_2

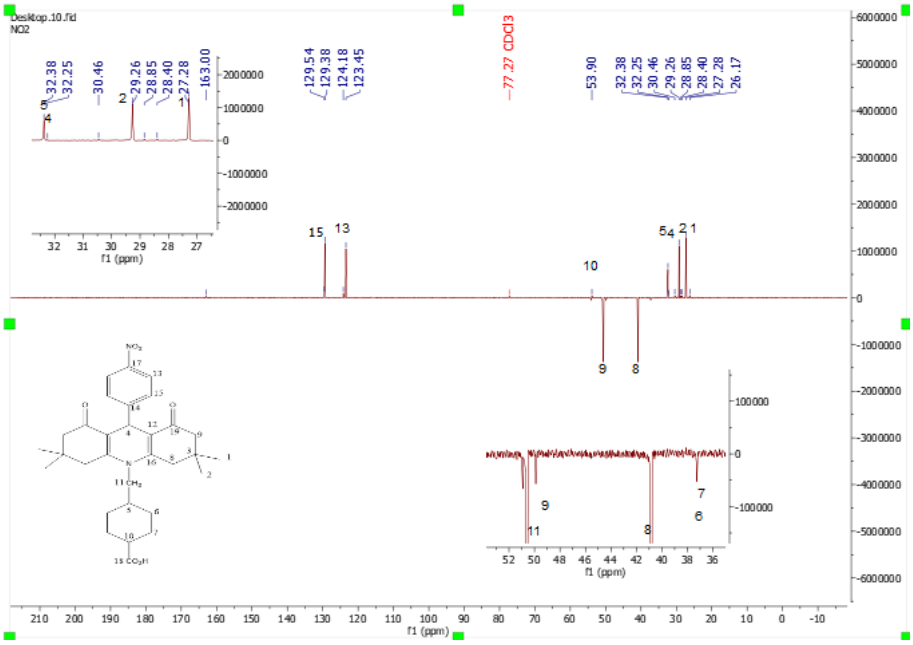

Figure 8. DEPT-135 spectrum of compound NO_2

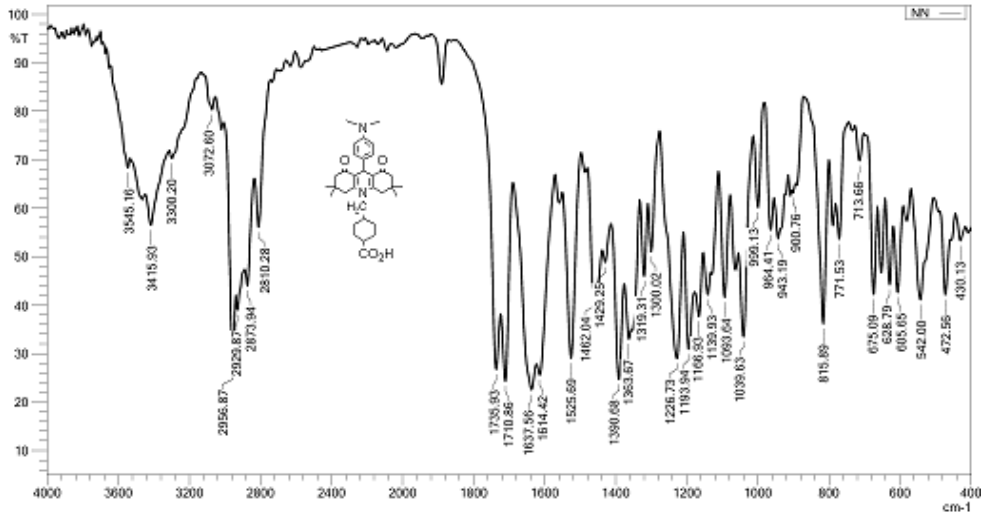

Figure 9. IR spectrum of compound NN

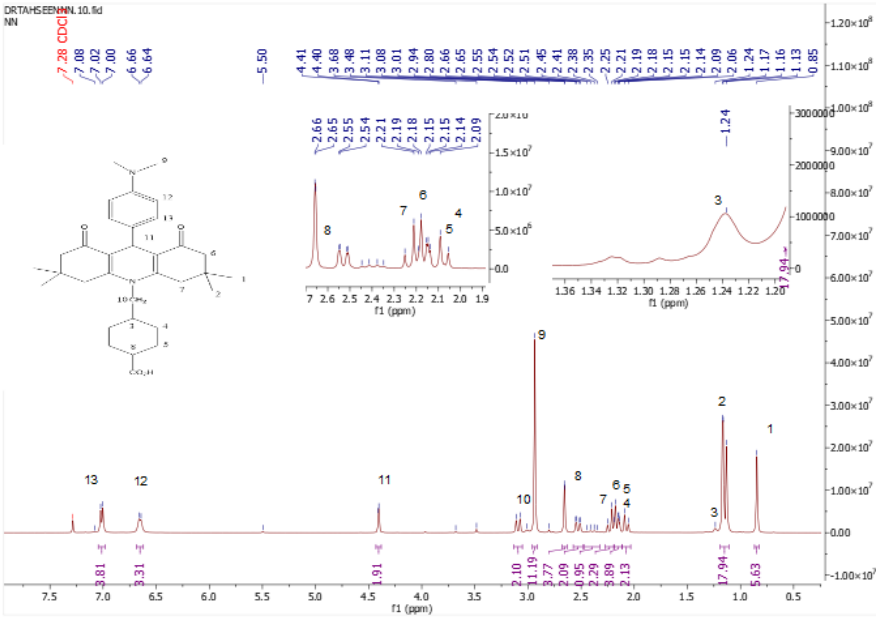

Figure 10. HNMR spectrum of compound NN

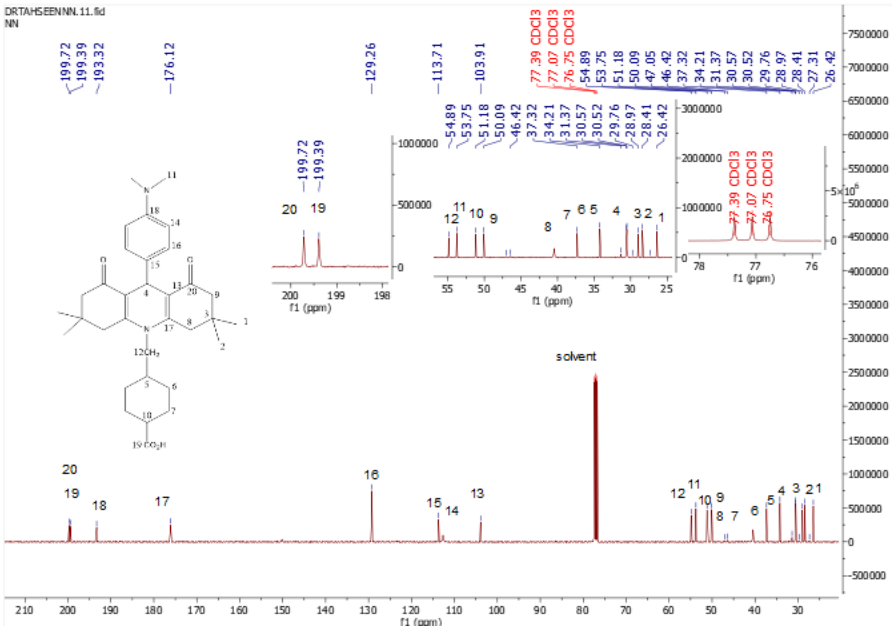

Figure 11. C^{13}NMR spectrum of compound NN

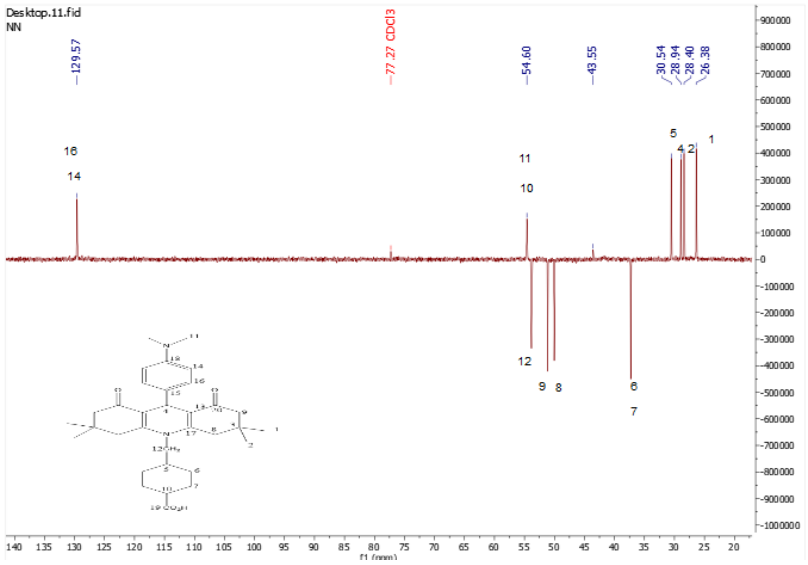

Figure 12. DEPT-135 spectrum of compound NN

References

Ahmad, H.M., Aldahham, B.J. & Saleh, M.Y. (2024). Dehydroepiandrosterone supplementation improves diminished ovarian reserve: Clinical and in silico studies. *Steroids*, 211, 109490.

AlHasan, L., Qi, A., Al-Aboodi, A., Rezk, A., Shilton, R.R., Chan, P.P., ... & Yeo, L. (2013). Surface acoustic streaming in microfluidic system for rapid multicellular tumor spheroids generation. In *Micro/Nano Materials, Devices and Systems*, 8923, 828-831.

Ali, A.H., Saleh, M.Y. & Owaid, K.A. (2023). Mild synthesis, characterization and application of some polythioester polymers catalyzed by cetrimide ionic liquid as a green and eco-friendly phase-transfer catalyst. *Iranian Journal of Catalysis*, *13*(1), 73-83. https://doi.org/10.30495/ijc.2023.1973500.1977

Ali, A.H., Saleh, M.Y., Yaqoob, Q.A., Saied, S.M., Hasan, M.S., Owaid, K.A. & Alsirhani, A.M. (2025). Comprehensive evaluation of antibacterial and anticancer activities from indole butanoic acid. *Journal of Genetic Engineering and Biotechnology*, *23*(1), 100452.

Ali, A.S., Al-Mathkuri, T.S.F. (2023). Synthesis and study of new pyrazoles and oxadiazole linked to the 1,4-dihydropyridine ring on breast cancer. *Journal of Chemical Health Risks*, *13*(4), 701-719. https://doi.org/10.22034/jchr.2023.1996251.1817

Ali, Z.H., Al-Saady, M.A.A.J., Aldujaili, N.H., Rabeea Banoon, S. & Abboodi, A. (2022). Evaluation of the antibacterial inhibitory activity of chitosan nanoparticles biosyntheseseized by streptococcus thermophilus. *Journal of Nanostructures*, *12*(3), 675-685.

Al-Jubori, H.M.S., Al-Mathkuri, F.T.S. (2022). Synthesis, characterization and biological activity of some heterocyclic compounds that derived from ibuprofen. *Egyptian Journal of Chemistry*, *65*(11), 795-802.

Al-Jubori, H.M.S., Al-Mathkuri, T.S.F., Banoon, Z.R. & Saleh, M.Y. (2024). Synthesis of novel benzo [d] imidazole bearing α-aminophosphonate and their antimicrobial evaluation. *Results in Chemistry*, 8, 101586.

Al-Mathkuri, F.T.S., Al-Jubori, H.M., Majed, A.A., Moker, M.H., Santali, E. & Alnajjar, R. (2025). Synthesis, breast cancer activity, molecular docking and dynamic simulation of 1, 4-dihydropyridine derivatives. *Journal of Molecular Structure*, 1321, 139704.

Al-Saady, A.J., Aldujaili, N.H., Banoon, S.R. & Al-Abboodi, A. (2022). Antimicrobial properties of nanoparticles in biofilms. *Revis Bionatura*, *7*(4), 71. http://dx.doi.org/10.21931/RB/2022.07.04.71

Al-Sultan, R.M.H., Al-Sultan, A.A., Hayawi, M.A., Aldahham, B.J., Saleh, M.Y. & Mohammed, H.A. (2022). The effect of subclinical thyroid dysfunction on B-type natriuretic peptide level. *Revis Bionatura, 7*(2), 21.

Al-Thakafy, N.T., Abdelzaher, M.A., Abdelzaher, H.G., Saleh, M.Y., Al-Enizzi, M.S., Saied, S.M. & Moghanm, F.S. (2024). A novel chalcone compound as a reagent for the validation of pharmaceutical cefotaxime sodium preparations. *Results in Chemistry*, 7, 101387.

Anchan, H.N., Ghate, M. & Joshi, S.D. (2023). Efficient synthesis of novel Biginelli and Hantzsch products. *ACS Omega, 8*(4), 3357-3366. https://doi.org/10.1021/acsomega.3c05106

Arif, A., Qureshi, M.S. & Ahmad, S. (2024). Synthesis of novel nitro-functionalized 1,4-dihydropyridines: A cost-effective, sustainable protocol with full spectroscopic characterization. *Journal of Molecular Structure*, 1305, 135241. https://doi.org/10.1016/j.molstruc.2024.135241

Assunta, C.M., Daniela, I., Roberto, R., Salvatore, V.G. & Laura, L. (2019). Recent developments in medicinal chemistry of bioactive molecules. *Current Medicinal Chemistry*, 26, 7166-7195.

Banoon, Z.R., Mahmood, R.S., Hamad, A.R. & Hussein, Z.A. (2025). Design, microwave synthesis, characterization and antimicrobial activity of imidazolone derivatives. *Journal of Molecular Structure*, 1322, 140701.

Bossert, F., Vater, W. (1989). Medicinal chemistry of dihydropyridines. *Medicinal Research Reviews, 9*(3), 291-324.

Breitenbucher, J.G., Figliozza, G. (2000). Efficient synthesis of bioactive heterocycles. *Tetrahedron Letters*, 47, 4311.

Dondoni, A., Massi, A., Minghini, E. & Bertolasi, V. (2004). Stereoselective synthesis of β-amino acids. *Tetrahedron*, 60, 2311.

Faizan, M., Khan, M. & Verma, A. (2024). Hantzsch reaction: The important key for pyridine and dihydropyridine synthesis - recent protocols and catalysts. *Synthetic Communications, 54*(1), 1-27. https://doi.org/10.1080/00397911.2023.2256785

Firouzabadi, H., Iranpoor, N. & Hazarkhani, H. (2001). One-pot synthesis of α,β-unsaturated carbonyl compounds. *Journal of Organic Chemistry*, 66, 7527.

Hamdoon, A.M., Al-Iraqi, M.A. & Saleh, M.Y. (2022). Synthesis of some multi-cyclic sulfhydryl donor compounds containing 1,2-dithiol-3-thione moiety. *Egyptian Journal of Chemistry, 65*(3), 427-434.

Hamdoon, A.M., Saleh, M.Y. (2022). Synthesis & biological evaluation of novel series of benzo [f] indazole derivatives. *Egyptian Journal of Chemistry, 65*(11), 305-312.

Hou, J., Kazemi, M. (2024). Recent advances on application nanomagnetic recoverable catalysts for synthesis of 1,4-dihydropyridine (DHPs). *Research on Chemical Intermediates, 50*(4), 1713-1743.

Ji, S.J., Jiang, Z.Q., Lu, J. & Loh, T.P. (2004). A new method for C–C bond formation in aqueous media. *Synlett*, 831.

Joshi, D., Milligan, J.C., Zeisner, T.U., O'Reilly, N., Diffley, J.F.X. & Papageorgiou, G. (2021). An improved method for the incorporation of fluoromethyl ketones into solid-phase peptide synthesis techniques. *RSC Advances, 11*(33), 20457-20464.

Kalaria, P.N., Karad, S.C. & Raval, D.K. (2018). Synthesis and biological evaluation of heterocyclic compounds. *European Journal of Medicinal Chemistry*, 158, 917-936.

Mathur, R., Negi, K.S., Shrivastava, R. & Nair, R. (2021). Recent developments in the nanomaterial-catalyzed green synthesis of structurally diverse 1, 4-dihydropyridines. *RSC Advances, 11*(3), 1376-1393.

Miri, R., Javidnia, K., Kebriaie-Zadeh, A., Niknahad, H., Shaygani, N., Semnanian, S. & Shafiee, A. (2003). Synthesis and evaluation of pharmacological activities of 3,5-dialkyl-1,4-dihydro-2,6-dimethyl-4-nitroimidazole-3,5-pyridine dicarboxylates. *Archives of Pharmacal Research*, 336, 422-428.

Miri, R., Javidnia, K., Sarkarzadeh, H. & Hemmateenejad, B. (2006). Synthesis, study of 3D structures and pharmacological activities of lipophilic nitroimidazolyl-1,4-

dihydropyridines as calcium channel antagonists. *Bioorganic & Medicinal Chemistry*, *14*(14), 4842-4849.

Ohberg, L., Westman, J. (2001). Synthesis of functionalized heterocycles via palladium-catalyzed reactions. *Synlett*, 1296.

Peri, R., Padmanabhan, S., Singh, S., Rutledge, A. & Triggle, D.J. (2000). Permanently charged chiral 1,4-dihydropyridines: Molecular probes of L-type calcium channels. *Journal of Medicinal Chemistry*, 43, 2906-2914.

Prabhakar, P.S., Sharma, N. & Raghavan, S.C. (2024). Aqueous solution of biogenic carboxylic acids as sustainable catalysts and green media for high-yielding synthesis of Biginelli adducts and 1,4-dihydropyridines. *RSC Advances*, *14*(2), 1053-1063. https://doi.org/10.1039/D4RA07772E

Rahimi, J., Karami, B., Eskandari, K. & Hosseini, S.H. (2022). Ammonium metavanadate (NH_4VO_3): A highly efficient and eco-friendly catalyst for one-pot synthesis of pyridines and 1,4-dihydropyridines. *Scientific Reports*, *12*(1), 13456. https://doi.org/10.1038/s41598-022-17378-7

Sadeek, G.T., Saeed, Z.F. & Saleh, M.Y. (2023). Synthesis and pharmacological profile of hydrazide compounds. *Research Journal of Pharmacy and Technology*, *16*(2), 975-982.

Safari, J., Banitaba, S.H. & Dehghan Khalili, S. (2011). Cobalt nanoparticles promoted highly efficient one-pot four-component synthesis of 1,4-dihydropyridines under solvent-free conditions. *Chinese Journal of Catalysis*, *32*(11-12), 1850-1855.

Saied, S.M., Mohammed, S.J., Khaleel, B.T. & Saleh, M. (2021). Comparative studies between conventional techniques and green chemistry to synthesis of novel piperidinium salts ionic liquids (PBSILs). *Journal of Chemical Health Risks*, *5*(4), 451.

Saied, S.M., Saleh, M.Y. & Hamdoon, A.M. (2022). Multicomponent synthesis of tetrahydrobenzo[a]xanthene and tetrahydrobenzo[a]acridine derivatives using sulfonated multi-walled carbon nanotubes as heterogeneous nanocatalysts. *Iranian Journal of Catalysis*, *12*(2), 189-205. https://doi.org/10.30495/IJC.2022.1955651.1924

Saleh, M.Y., Al-barwari, A.S. & Ayoob, A.I. (2022). Synthesis of some novel 1,8-naphthyridine chalcones as antibacterial agents. *Journal of Nanostructures*, *12*(3), 598-606.

Saleh, M.Y., Aldulaimi, A.K.O., Saeed, S.M. & Adhab, A.H. (2024). $TiFe_2O_4$@SiO_2-SO_3H: A novel and effective catalyst for esterification reaction. *Heliyon*, *10*(4), e26286.

Saleh, M.Y., Aldulaimi, A.K.O., Saeed, S.M. & Adhab, A.H. (2025). Palladium fabricated on Fe_3O_4 as an organic - inorganic hybrid nanocatalyst for the Suzuki and Stille coupling reactions. *Journal of Molecular Structure*, 1321, 139597.

Shan, Y., Su, L., Zhao, Z. & Chen, D. (2021). Transition-metal catalysis in organic synthesis. *Advanced Synthesis & Catalysis*, 363, 906-923.

Singh, J., Abraham, R. (2023). Investigation and application of 2-(benzyloxy)-4,5-diphenyl-1H-imidazole as an anti-inflammatory and analgesic agent. *Biological and Molecular Chemistry*, *1*(1), 27-34.

Voigt, B., Coburger, C., Monar, J. & Hilgeroth, A. (2007). Structure - activity analysis of novel N-acyloxy-1,4-dihydropyridines as P-glycoprotein inhibitors. *Bioorganic & Medicinal Chemistry*, *15*(15), 5110-5113.

Zhou, X., Zhang, L., Tseng, E., Scott-Ramsay, E., Schentag, J.J., Coburn, R.A. & Morris, M.E. (2005). New 4-aryl-1,4-dihydropyridines and 4-arylpyridines as P-glycoprotein inhibitors. *Drug Metabolism and Disposition*, *33*(3), 321-328.

Zolfigol, M.A., Salehi, P. & Safaiee, M. (2006). An efficient and eco-friendly procedure for the synthesis of Hantzsch ethyl 1,4-dihydro-2,6-dimethylpyridine-3,5-dicarboxylates under mild and green conditions. *Letters in Organic Chemistry*, 3, 153-156.

Żorniak, M., Mitręga, K. & Krzemiński, T.F. (2011). Cardiovascular safety in pharmacological treatments. *Polish Heart Journal*, 3, 100-103.